Ceramics International xxx (xxxx) xxx–xxx

Contents lists available at ScienceDirect

Ceramics International

journal homepage: www.elsevier.com/locate/ceramint

Surface modification of orthopedic implants by optimized fluorine-substituted hydroxyapatite coating: Enhancing corrosion behavior and cell function

Mojtaba Mansoorianfar[a], Mostafa Mansourianfar[b], Mohammadhossein Fathi[c], Shahin Bonakdar[d], Mohsen Ebrahimi[a], Ehsan Mohammadi Zahrani[c], Hojjati-Najafabadi Akbar[e,*], Li Dagang[a,**]

[a] College of Materials Science and Engineering, Nanjing Forestry University, No. 159, Longpan Road, Nanjing, 210037, Jiangsu, PR China
[b] Faculty of Environment, University of Tehran, Iran
[c] Department of Materials Science and Engineering, Isfahan University of Technology, Isfahan, Iran
[d] National Cell Bank, Pasteur Institute, 1316943551, Tehran, Iran
[e] Faculty of Materials, Metallurgy and Chemistry, School of Materials Science and Engineering, Jiangxi University of Science and Technology, Ganzhou, 341000, PR China

ARTICLE INFO

Keywords:
Fluorhydroxyapatite
Nano-porous
Biocompatibility
ALP activity
Osteoblast cell (MG-63)
Corrosion properties

ABSTRACT

Fluorine may only have negative effects on bone metabolism if the optimum concentration of fluorine would not be determined, especially in osteoporosis. In this study a nano-porous and uniform fluorhydroxyapatite (FA) coating in different concentration of fluorine could be deposited on the 316 L substrate with a thickness of 50 μm. Fluorine can have influence on cell proliferation, matrix production, ALP releasing, coating dissolution rate, bio activity, and corrosion resistivity. The dissolution rate of the coating evaluated by ICP and found with an increase in fluorine due to the elimination of CaO, Ca^{2+} releasing decreased. The results of SBF and MTT exhibited the fluorine within the apatite structure enhanced the growth of natural apatite and function of human osteoblast like cell (MG-63). Furthermore, cell density and attachment showed an enhancement while fluorine increased. Surprisingly the ALP activity test showed the mineralization ability of coating would be improved significantly in presence of fluorine. Furthermore potentiodynamic polarization showed with increasing fluorine, the current density decreased from 112 to 13 nA/cm^2. Corrosion property of FA is higher because it is too stable but can also persuade to severe adverse effects like osteomalacia. According to the achieved results, 75% partially-substituted fluorine within apatite structure was introduced as a proper combination of biocompatibility while 100% substituted fluorine could be a better candidate in corrosion resistant performance.

1. Introduction

Hydroxyapatite (HA), is represented with the chemical formula of Ca_{10} $(PO_4)_6$ $(OH)_2$ and serves as an essential substance for bone and tooth implants due to its chemical composition which is similar to the bone tissue [1–3]. The degradibility of apatite is one of the most critical factors as its solubility would give better bioactivity for bone healing though it lowers the mechanical strength [4,5]. However, if HA was applied as a coating on an implant, the constructed bonding between the implant and newly grown bone could be unstable due to its solubility, accordingly, the function of the coating is degraded [6,7]. Hence, it is critical for bioactive coating to have acceptable and reasonable solubility. The degradability of bioactive coatings can be controlled by some variables such as the stoichiometry, degree of crystallinity, and composition. The substitution of fluorine (F^-) instead of OH^- group in HA chemical structure is an actual way to decrease the solubility of apatite. In fact, fluorine has been shown to be effective in stimulation of osteoblastic activities regarding cell proliferation and differentiation [7–11]. The FA forms a solid solution with HA to form fluorhydroxyapatite [FA, Ca_{10} $(PO_4)_6$ $(OH,F)_2$] by substitution of OH^- with F^-. By increasing the fluoride ion content in apatite structure the hydroxyl-fluorine bonds appear while hydroxyl and hydroxyl-fluorine-hydroxyl bonds disappears significantly. Therefore in fully fluorine substitution there is no hydroxyl band. In our previous researches we proved there was sufficient binding of fluoride to overcome hydroxyl bonds. Also due to the applied strain on the apatite structure caused by fluorine substitution the crystal structure of apatite shrinks and Ca–P and P–O bonds come near together [12]. Since ALP increases in fluorine therapy

* Corresponding author.
** Corresponding author.
E-mail addresses: a_hojjati@yahoo.com (A. Hojjati-Najafabadi), njfuldg@163.com (D. Li).

https://doi.org/10.1016/j.ceramint.2019.09.197
Received 25 August 2019; Received in revised form 14 September 2019; Accepted 20 September 2019

for osteoporosis, it is commonly accepted that fluorine encourages bone formation. However, histochemical studies have revealed that osteocytes resorbing also increase ALP enzyme. Many studies recommended that an increase of ALP and bone mass following fluorine therapy signify a failed repair reaction rising in both bone formation and resorption. This repair reaction to cell injury is the result from pathological bone formation [13–15]. Furthermore, while the repair process fails a toxic death of resorbing osteocytes and a reduction in bone resorption happens. Osteoclasia of fluorotic bone results in further toxic effects to decrease bone resorption by fluorine affected osteoclast cells [16]. L. Krook et al. [17]. by using pathological bone formation showed that the enlarged amount of trabecular bone comes from suppressed bone resorption by resorbing osteocytes and osteoclasts and damaged osteoblasts. Both resorptive processes are mandatory for the restoration of trabecular bone into compact bone. A skeletal disorder described by bone strength which is prone to increased risk of fracture is named osteoporosis. In osteoporosis abnormality in bone cell behavior forms insufficient bone matrix. Fluorine is an element essential for skeletal and dental activities by reducing tooth cavities and generating a hard tissue similar to the bone. Also it inspires the formation of bone and can develop the quality of newly formed bone by encouraging the formation of crystalized hydroxyapatite [18]. Fluorine may only have negative effects on bone metabolism if the optimum concentration of fluorine would not be determined, especially in osteoporosis. Rockvile et al. [18] showed that the amount of 10^{-5}-10^{-7} M of fluorine could be useful and optimum for the effective role of fluorine. The process of building the skeleton by osteoblasts and osteoclasts cells is named modeling and remodeling. During our life bones are sculpted by modeling process, which forms new bone at one site. Remodeling is an interaction between osteoblasts and osteoclasts. It is critically important to understand, since the remodeling is the main method of bone reshaping in adults and treatment of bone malformations and bone abnormalities [18] Fig. 1 shows the schematic of modeling process, mesenchymal stem cells differentiation and bone healing in presence of fluorine in a tiny crack in the bone.

The main advantages of Sol–gel such as chemical composition control and low-temperature have made this technique well known to synthesize various thin film coatings and materials [7,20,21]. Also, sol-gel technique shows wonderful potential to prepare bioactive materials. Many studies [10,11,22,42] have focused on preparation of FA coating, formation mechanism and some invitro tests. For many years, using of fluorine as an useful element in orthopedic implants as powder, crushed substances, and coating have been more attractive for scientists. Many researches have been done on the effect of fluorine on enhancing biological abilities [24], mechanical and bioactivity properties [25,26] and solubility of fluorine -substituted hydroxyapatite [27]. But there are no specific study on specifying the optimum concentration of fluorine in point view of formation, biobehavioral and corrosion properties. The meager dissolution rate of FA in biological applications was also reported [7]. Nonetheless, unaided FA may not be a suitable biomaterial because it is too stable and it does not have good enough biological properties. Therefore, to achieve the optimum bioactivity of the material it is necessary to optimise the fluorine content in fluorine-substituted HA. To fill this knowledge gap in this study a process for the generation of suitable FA coating by sol-gel method in the presence of the optimum fluorine incorporation in HA structure and evaluation of solubility, toxicity, osteoblast cells function, and corrosion properties of coating have been investigated.

2. Materials and methods

FA coating was applied using the sol-gel method accordingly. Phosphorous pentoxide (P_2O_5, Aldrich), calcium nitrate tetrahydrate ($Ca(NO_3)_2{\cdot}4H_2O$, Merck); and hexafluorophosphoric acid (HPF_6, Aldrich) were considered as P; Ca and F precursor, respectively. In preparing the solutions, $Ca(NO_3)_2{\cdot}4H_2O$ and P_2O_5 were dissolved in absolute ethanol (Merck); separately. Afterwards, HPF_6 was poured in that mix suspension. A designed amount of fluorine, P^-, and Ca^{2+} precursors were mixed with containing ethanol solution to form a mixture to obtain Ca/P and Ca/F ratios of 1.67 and 5 to 20, respectively. Herein, the fluorine substituted samples are designated as HA (0% F), FA25 (25% F), FA50 (50%F), FA75 (75%F), FA (100%F). This mixed solution was stirred for 24 h at a speed of 1300 rpm to obtain the sol. The 316 L stainless steel (st.st) sheet as a substrate was cut to desired dimensions (20 × 30 × 3 mm). Grounding up to 2400 grit sand papers, polishing and ultrasonication in acetone for 15 min applied on the specimens before dip coating, followed by washing in deionized water. The samples held by a computerized holder at a speed of V = 1 mm/s were dipped into the sol with θ = 45° and withdrawn with 40 s total soaking time. Dipping process was done before gelation because experiments showed gelation occurs after 3 h and after the addition of a final element to the sol. The as-dipped coating was dried at 120 °C for 24 h followed by heat treatment at a rate of 3 °C/min up to 600 °C and then cured at 600 °C for 1 h. The first step after sol preparation was sufficient polymerization to making up the skeletal structure by forming molecules cross-linking [7]. The final step was

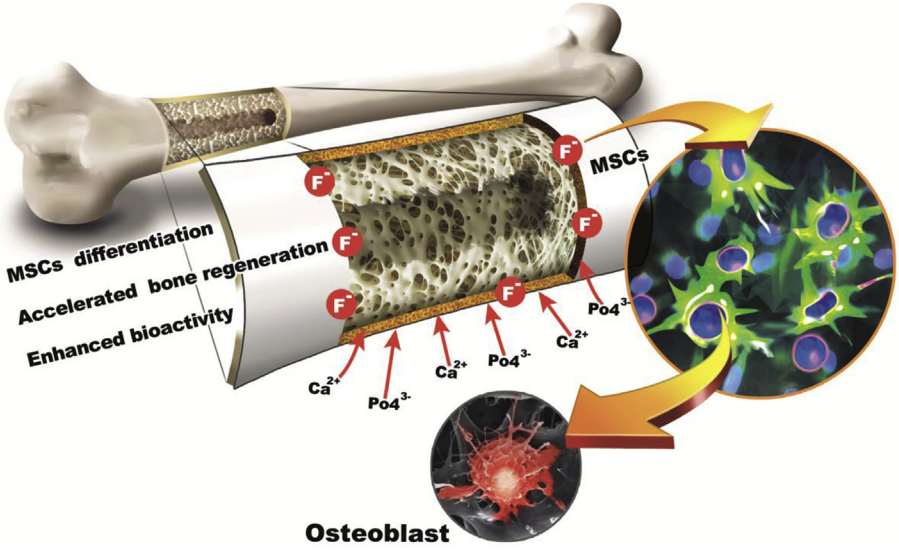

Fig. 1. Schematic of the fluorhydroxyapatite (FA) tissue used in this study and surface engineered thin film of FA.

coating, drying, and heat treatment to crystallized the coating. Dissolution rate of the films was measured by immersion in simulated body fluid (SBF) and aged for predetermined periods of time. At several incubation periods up to 28 days, Inductively Coupled Plasma-Atomic Emission Spectroscopy (ICP-AES; ICPS-100IV, Shimadzu, Japan) was used to measure the concentration of the Ca ions released from the film. HA coatings were also tested as control sample. After 28 days, the FA coatings take out from SBF solution to characterize with an X-ray diffractometer (Philips X Pert-MPD system using mono-chromatized CuKα radiation) at a scanning speed of 0.02°/sec. Further Scanning Electron Microscope (SEM, Philips XL30) was used for monitoring surface morphology and thickness.

Osteoblast cell with an incubation time of 3 and 7 days in a protocol based on ISO 10,993-5 was utilized for MTT assay. Prior to cell seeding, the coatings were sterilized then some RPMI medium without FBS was added to the samples to cover their surface. After 1, 3 and 7 days of incubation, the soup was placed in a 96-well culture plate; osteoblast (MG-63) (from Shanghai Cell Bank), medium RPMI supplemented with 10% FBS, and penicillin-streptomycin were added into the wells and incubated in a humified incubator for 1 day with 5% CO_2 atmosphere at 37 °C. MTT solution was added to each sample and incubated at 37 °C for 4 h. Then, isopropanol was added to the samples and absorbance of each samples was measured [28,29]. The ALP test was performed within 1, 3 and 7 days. To extract protein from the cell, the supernatant was centrifuged with rate of 13,000 rpm for 15 min after adding 200 µl of Rypa buffer. Then 50 µl of the supernatant was poured into a 96-wells plate and 150 µl of alkaline phosphatase (ALP) kit (Solarbio, China) was added with ratio of 4/1. The ELISA reader was performed at wavelength of 450 nm to measure the ALP activity.

Potentiodynamic polarization tests were measured by an EG&G 2273 A potentiostat instrument. Polarizing the specimens by using open current potential value (EOCP) was performed from −400 to 600 mV at scanning rate of 2 mVs^{-1}. The corrosion current (I_{corr}) values are related to a 50 mV stretch among the anodic and cathodic parts of the resulted polarization curve. To evaluate the corrosion performance, electrochemical impedance spectroscopy (EIS) of the FA films were measured on 316 L panel. The frequency range of sinusoidal perturbations was considered 10^{-1}-10^{5} Hz while applying 5 mV at open circuit potential (OCP). A three-electrode cell equipped with Ag/AgCl reference electrode, platinum counter electrode and a coated 316 L substrate as the working electrode ensuring an exposed area of ~1 cm^2. All measurements were carried out in 37 °C Ringer's solution and in order to reproducibility were repeated three times.

3. Results and discussion

3.1. Structural characterization of coating

To prepare sol a two-step procedure was employed in sol preparation: one hydrolyzation in water and the subsequent reaction is Ca involvement that is critical in developing a desirable apatitic structure [11]. When the precursors mix up together, hydrolysis reaction with no ion interaction takes place. But, after enough time sol converts to gel the ion interactions increase and hydrolysis interactions are completed to release organic components and volatile gases from the sol [42]. In Fig. 2. SEM results showed nano size holes of 100–400 nm on the surface of coating which have generated by volatile gases and incomplete polymerization reaction. Because of their roles as the initiate points for apatite growth, these holes can be useful for osteoconduction [30]. However, large quantity of holes is not suitable for the mechanical strength of coating, so by controlling the parameters, appropriate micro and nano holes can be obtained. These pores look like the holes formerly reported by Kim et al. [31]. According to the theory which was mentioned, aging helps the sol to complete its reaction and prevent creation of unwanted phases [42]. Comparison made between Fig. 2 demonstrated that aging time can be useful in morphology and quality of the surface.

Thermal expansion coefficient can be more critical point in heat treatment process. Differences of this coefficient between the coating and base metal cause to cracks and layer delaminating while drying and hat treatment [32]. Increasing the soaking time, increase the thickness of coating and probability of delaminating but it would be stable in specific time. In Fig. 3 the slim shift of the characteristic (211) peak to the right was associated to the decrease of the a-axis of the hexagonal HA crystal lattice. This statement was acceptable when it was recognized that fluorine has not tendency to effect the lattice parameter "c", but superficially decreases the lattice parameter "a".

Lattice parameter calculation showed the replacement of fluorine with hydroxyethyl groups, which has larger ion radius than fluorine, changed the lattice parameter “a" but no change in lattice parameter “c" was observed (Table 1). This substitution in excess of 25% of fluorine causes a contraction in the crystalline FA lattice. The lattice parameters “a" and “c" of FA crystal with different percentages of fluorine replacement, which were calculated using the data obtained from the XRD, are presented in Table 1. It is obvious that with the increase of fluorine replacement in the structure of FA, the lattice parameter would be decreased. At the same time, almost the same values for the lattice parameter “c" in all of the fluorine replacement percentages were calculated, which indicates that the presence of fluorine in the apatite structure didn't effect on lattice parameter “c". There is not effective change in the c-axis direction by fluorine substitution in the apatite structure because by increasing fluorine ion the lattice strain decreases due to the lower ionic radius of fluorine than OH^- ion. The c-axis lattice parameter in this study was estimated about c = 0.6881 nm which was corresponded to other researches which had been around c = 0.6884 nm [12,33]. This result is in harmony with a slight shift of characteristic peak to higher diffraction angles, resulted from an increase in the presence of fluorine. Also the peaks of the FA were severer than HA. Therefore, it can be understood that the crystallinity of the crystals is enhanced by fluorine incorporation into the HA matrix [34]. The higher crystallinity causes higher thermal and chemical stability of FA [20].

The dissolution rate in SBF media is different for some calcium phosphate phases such as tricalcium phosphate ($Ca_3(PO_4)_2$, TCP, α-TCP, β-TCP), tetracalcium phosphate ($Ca_4P_2O_9$, TTCP), calcium oxide (CaO), oxyhydroxyapatite (OHA), amorphous Hydroxyapatite (ACP) and oxyapatite (OA). Comparing of the dissolution rate of these phases shows CaO > TCP > ACP > TTCP > OHA = OA > HA. Among these phases, CaO can be dissolved considerably faster than other phases [42,30,35]. According to Fig. 3 in FA25 some CaO content exists in structure which promotes dissolution rate of FA25 rather than other samples. The dissolution of this unstable phase in the coating leads to a better bioactivity but undesirable reduction of the mechanical strength [11].

With the purpose of observing the dissolution behavior of the films, the FA films deposited on substrate after heat treatment were immersed in SBF solution. At each period of time, the samples were taken from SBF and the concentration of the dissolved Ca^{+2} ions was determined using ICP. During the soaking time of the coating in SBF solution, the releasing rate of Ca^{+2} increases, but it decreased with an increase in fluorine concentration (Fig. 4). The FA layer suggests the tailoring of solubility with fluorine substitution within the apatite structure resulting lower solubility than HA. In Fig. 4. FA25 has some CaO content which promotes dissolution rate of FA25 rather than the others because CaO dissolves significantly faster than the other phases. Therefore, the ion release profiles in FA25 and HA are close together.

Note to the crystalline structure of HA a certain degree of disordering comes out when hydrogen (H^+) and oxygen (O_2^-) ions are arranged beside together to form OH^- group; randomly. Once the OH^- is partially substituted by the fluorine, due to the greater affinity of fluorine rather than oxygen, the hydrogen ion of the OH^- group is bound to the closer fluorine because of the, producing a fully well-

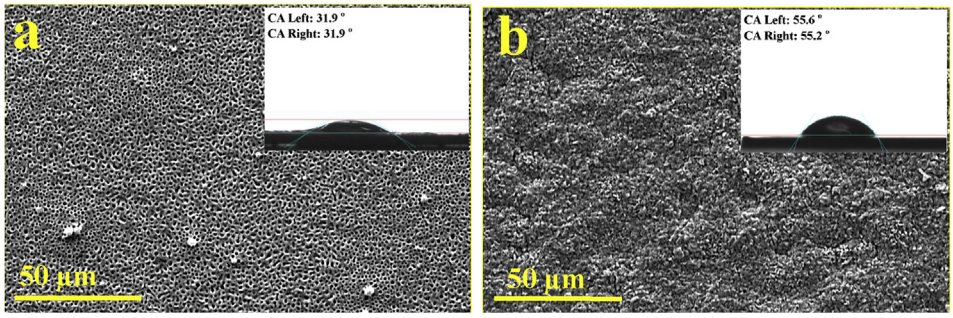

Fig. 2. SEM morphology of the calcined FA coating at 600 °C a) before aging, b) after 24 h aging.

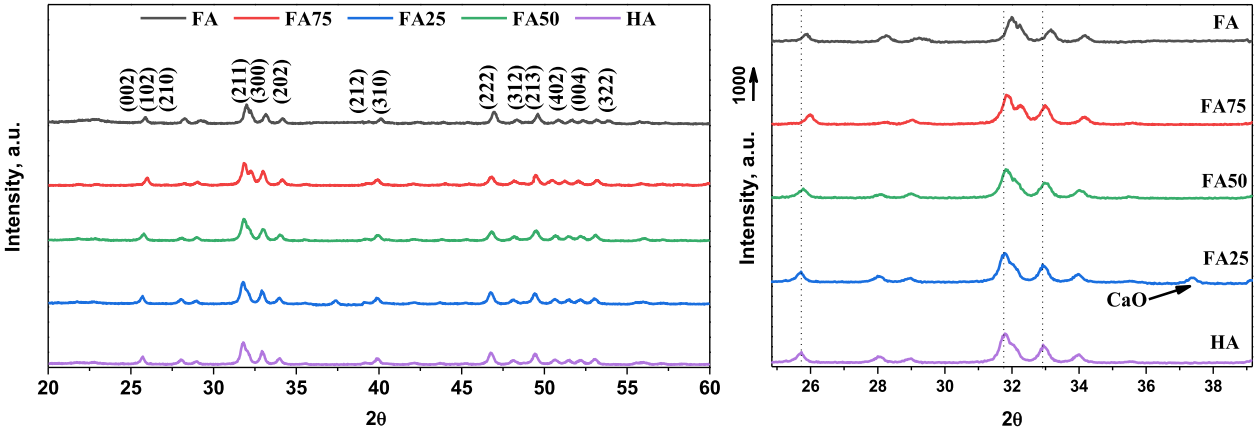

Fig. 3. XRD pattern of coating after calcination at 600 °C.

Table 1
Variation of lattice parameters of FA in different fluorine substitution.

	d (nm)	*c*-axis (nm)	*a*-axis (nm)
HA	41.48	0.688	0.941
FA25	42.05	0.688	0.939
FA50	44.98	0.688	0.938
FA75	46.20	0.688	0.937
FA	46.54	0.688	0.937

ordered apatite structure, affecting the thermal and chemical stability. Henceforth, an assured level of thermal, corrosion and chemical stability of the FA is attained when a specified amount of fluorine replaces with the OH^- groups in the HA matrix [7,9]. Fig. 4 showed during the early days of incubation the rate of fluorine concentration decreased over time.

3.2. In-vitro characterization of coating

The apatite formation in SBF solution is as an indicator to measure bioactivity of a substance [36]. The presence of Ca^{+2} and PO_4^{-3} in SBF solution triggered the formation of apatite on the specimen. The influence of the presence of fluorine on HA formation in SBF solution was monitored after 28 days. Due to the higher degradability of HA during incubation in SBF solution, the formation of apatite was satisfactory. With an increase in fluorine into HA structure, degradability of HA decreased; therefore, the coating had low saturation rate rather than HA in a pure state, so nucleation of apatite decreased remarkably (Fig. 5). At the first step due to the extra negative charge on the surface of FA rather than HA (due to the stronger electronegativity of fluorine compared to OH), the apatite formation in SBF gets faster. This negative charge of the surface attracts calcium from medium to form the Ca-rich ACP phase, and then impose positive charge on the surface. At the second step, the Ca-rich ACP on the surface motivates the negative

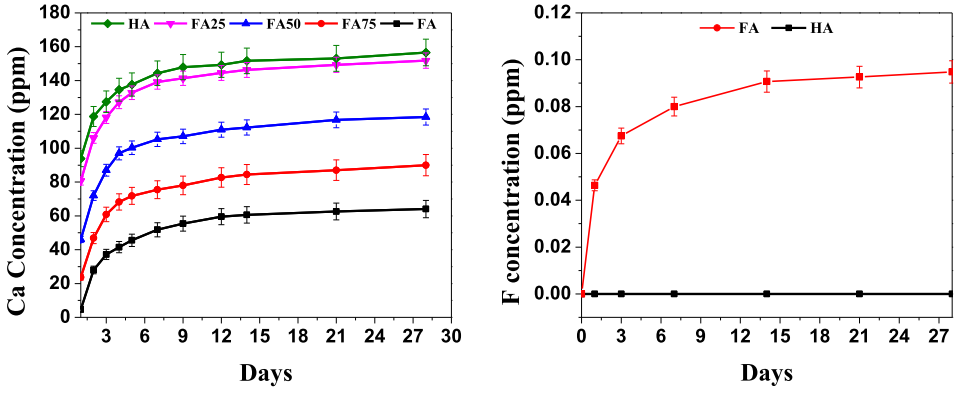

Fig. 4. Dissolution behavior of Ca and fluorine after soaking in SBF solution for 28 days.

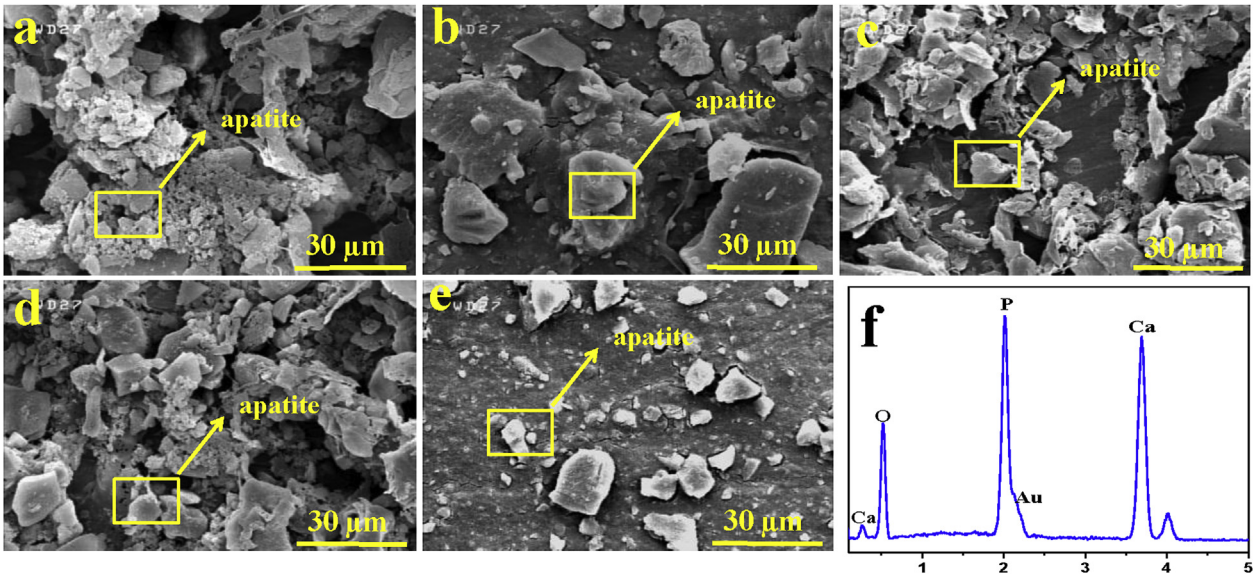

Fig. 5. SEM images of films after 28 days of incubation in the SBF solution: **(a)** HA; **(b)** FA25; **(c)** FA50; **(d)** FA75; **(e)** FA.

charge phosphate ion from medium to make Ca-poor ACP and gradually apatite could nucleate and grow on the surface. By the way it can be concluded that biocompatibility and rate of osteogenesis significantly increase in presence of fluorine rather than natural hydroxyapatite [37].

MTT and ALP release evaluation under the presence of fluorine were performed and reported in Fig. 6. MTT results in Fig. 6a proved there is no toxicity existed in the sample with fluorine in comparison with HA sample. Also due to the appropriate chemical composition it showed an enhanced cell viability of the coatings. It seems that the cell viability of the osteoblast cell enhanced; accordingly, the coating can be more appropriate for bone tissue applications. Fig. 6b shows the ALP activity results obtained from cell cultured FA coating in various fluorine concentration. The ALP activity increases slightly in presence of fluorine. The most important point is increasing of ALP does not necessarily indicate bone growth and stimulation of osteoblast cells. The concept that fluorine as a specific stimulus for bone application is preposterous because fluorine is a potent enzyme poison [38]. Instead, repairing reactions against cell damaging of osteoblasts and osteocytes caused by fluorine increases ALP production. The repairing reaction followed by enhancing of osteoblasts proliferation, matrix and ALP production. Any failure in repairing reactions for osteoblastic cells, carries either apoptosis or necrosis, and disrupts proliferation of osteoprogenitor cells. This repair and cell death process proceeds until the fluorine concentration reaches the appropriate level. These new osteoblasts will then be damaged, and the cycle of increased would be repeated. This motivation of the repair reaction in osteoblasts would contribute to ALP [39,40].

To evaluate the biocompatibility of the fluorine incorporated within the apatite structure, beside MTT and ALP assays the cell-cell and cell-matrix contacts also is necessary. Cell attachment evaluation was examined on the MG-63 osteosarcoma cells because osteoblast tissue is in directly contact with the implant, besides, they are extremely proliferative. Actually in this research we have supposed our implant as a substance which is in bone contacts. In this point of view coating and tissue contact joints both osteoblast and fibroblast cells are participated but for evaluation of toxicity by MTT even one of which is enough. We have investigated this in our previous study [29]. Cell attachment showed an improved cell viability of the fluoride HA (Fig. 7). Moreover, the highest concentration of cell was reached in FA75. In fact, the good cell attachment can also be related to the released fluorine concentration which excites the activity and proliferation of osteoblast cells.

Fig. 8a illustrates the potentiodynamic curves and corrosion current density (I_{corr}) values of the whole series of the FA specimens with different fluorine concentrations. (Summarized in Table 2). As results proved FA specimen showed the lower I_{corr} value than others. Generally, lower I_{corr} values for fluorine substituted coating compared to the HA coated ones indicates that FA coatings play a role as a physical barrier to avoid chemical reaction between substrate and physiological solution. Also, the presence of micro cracks and voids in HA which debilitates the barrier capability of HA coating. Biodegradability is another factor which effects on corrosion current density [41]. As noticed in previous section, due to biodegradability decreased by increasing fluorine incorporation within the apatite structure, therefore

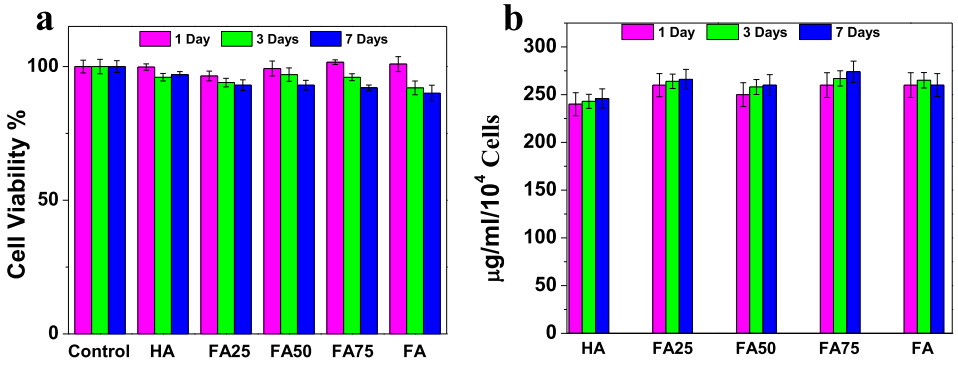

Fig. 6. a) Cell viability of FA film coating containing various F^-, b) ALP of FA film coating containing various fluorine.

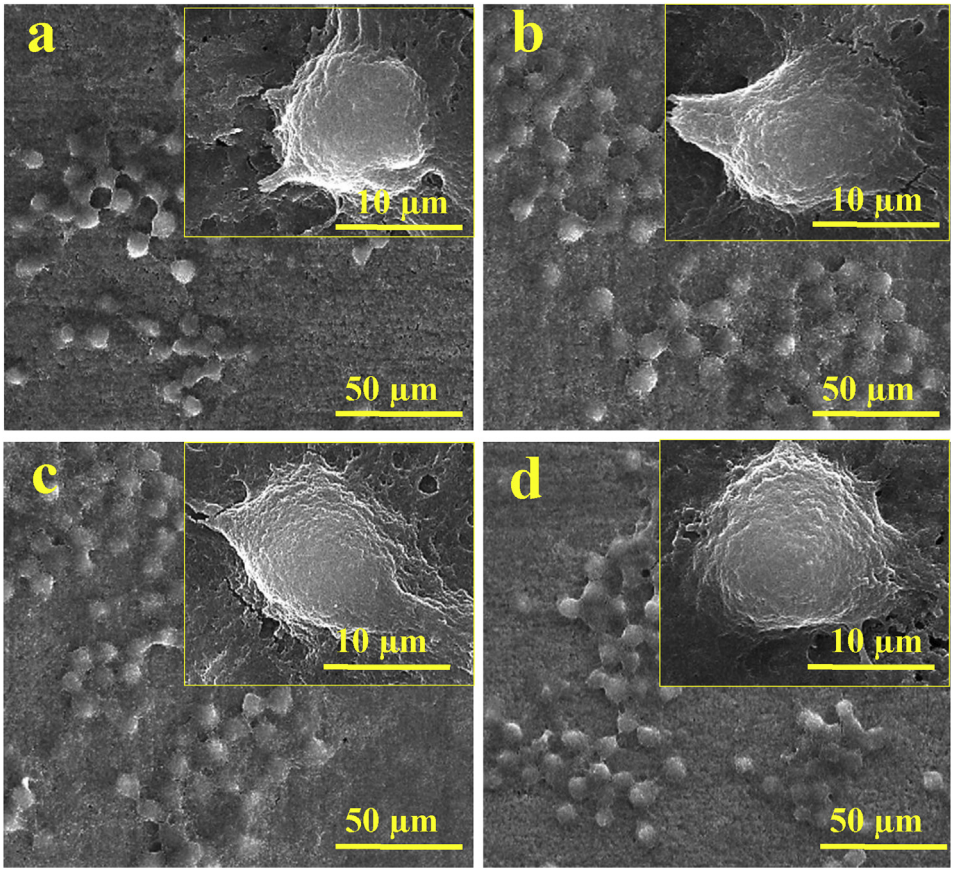

Fig. 7. The SEM images of MG-63 bone marrow stromal cell cultured (after 1 days) on (a) FA25, (b) FA50, (c) FA75 and (d) FA.

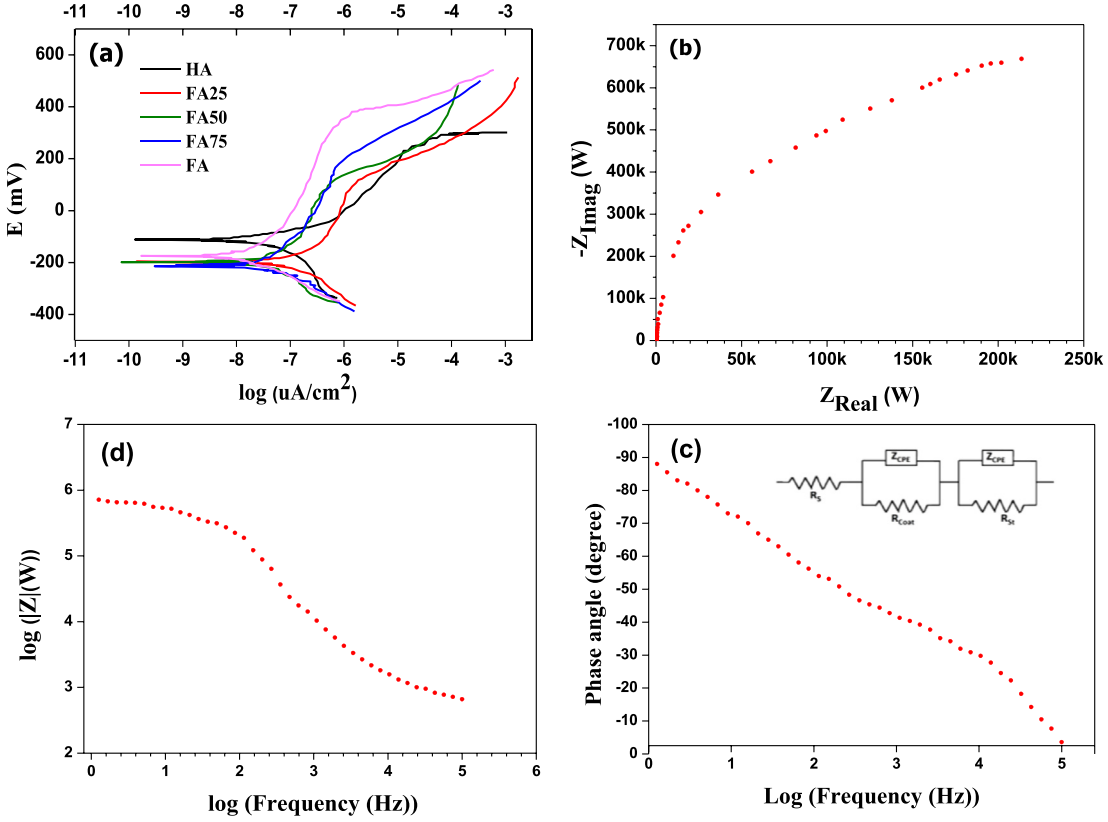

Fig. 8. a) Potentiodynamic polarization recording curves at ringer solution in 37 °C for FA with different fluorine content, b) Nyquist plot for FA after immersing in ringer solution for 30 min, c and d) Bode plots for FA after immersing in ringer solution for 30 min. Inset represent equivalent circuit used to model impedance curve.

Table 2
Electrochemical characteristics for FA in different ratio of fluorine on 316 L substrate.

	HA	FA25	FA50	FA75	FA
E_{corr} (mV)	−75	−130	−197	−201	−109
I_{corr} (nA/cm^2)	112.2	41.98	30.90	26.30	13.18

Table 3
Impedance parameters for FA coated on 316 L substrate.

Sample	R_s (Ω)	R_{coat} (Ω)	Z_{CPE}^{coat} (F.s)
FA	17.59 ± 0.11	6.67E6 ± 0.24E6	29.73E-6 ± 2.978E-7
n_{coat}	R_{St} (Ω)	Z_{CPE}^{St} (F.s)	n_{St}
0.780 ± 0.012	76.41 ± 0.38	138.51E-3 ± 5.415E-4	0.97 ± 0.05

corrosion rate could be decreased, and FA coated samples show good corrosion properties in comparison to HA coated sample. In FA passivated sample up to −110 mV and HA sample proved maximum corrosion potential (E_{corr}) compared to fluorine incorporation within the apatite structure. Moreover, for taking deeper corrosion characterizations, AC impedance analysis was carried out for FA coated sample. Fig. 8b displays the Nyquist and Fig. 8c & d illustrate Bode plots for FA after 30 min of immersion. It is well known that with a significant releasing the metal ions around tissues caused to biological damage in short or prolong periods. Hence, if the amount of Rcoat (6.67 × 106 Ω) is larger than R_{st} (76.41 Ω), the corrosion resistance will be improved, or corrosion rate will be decreased. Thus, the plausible mechanism for better corrosion resistance of FA on 316 L is suggested by creating a stable corrosion barrier on substrate. Bode plots diagram of FA coated sample after dipping for 30 min are illustrated in Fig. 8c & d. As concluded in Fig. 8c, with increasing impedance modulus $|Z|$ at lower frequencies, the corrosion rate decreased. On the other hand, the second type of bode plots revealed that the impedance spectrum of FA is wide phase angle at whole frequencies which is attributed to both of forming a stable film and presence of barrier coating. The numerical fitting was used to interpret the impedance spectrum. To describe the deviations from ideal behavior, a constant phase element (CPE) was performed instead of an ideal capacitor. The CPE impedance (Z_{CPE}) well defined by $Z_{CPE} = 1/Y\ (\omega j)^n$. Where Y is pseudo-capacitance, ω is the frequency, and n is a parameter which related to the homogeneity of system. The exp(n) is lower than one for CPE. R_s and R_{coat} are the resistance of electrolyte and the resistance of the FA coating, respectively. R_{St} and R_{ct} are pseudo-capacitance contributed to the thin natural FA oxide film and the resistance which explaining the corrosion of metal substrate, respectively. Equivalent circuit used to model impedance curve has been demonstrated in the inset to Fig. 8d. The data fitting for this model has been also summarized in Table 3. According to the inset to Fig. 8d, as two phase constants are series, a barrier coating has been created that it can be protected the substrate against corrosion.

4. Conclusion

- The added fluorine incorporated within the apatite structure confirmed by lattice parameter measurements. Addition of fluorine in HA lattice decreased the lattice parameter “a" while there was no variation in the lattice parameter “c".
- The dissolved Ca, P ions varied as a function of fluorine concentration in HA lattice by measuring dissolution behavior of the FA coating. With presence of fluorine in FA, the releasing rate of calcium and phosphor ion, decreased.
- The formation of agglomerated HA particles on the coatings has been revealed after 28 days of incubation during SBF test. Due to the higher affinity of F^- rather OH^- in ion adsorption from media the formation of apatite enhanced without a change in the size, morphology, and composition of the apatite.
- In FA25 some CaO content exists in structure which promotes dissolution rate of FA25 rather than the others. Among calcium phosphate compositions, CaO dissolves significantly faster than the others.
- MTT and ALP assay after 1, 3, 7 days of incubation using osteoblast cells showed that FA75 has higher viability and ALP release. However, cell morphology and attachment on FA75 better than others.
- The corrosion properties indicated that with increasing fluorine within the apatite structure, the corrosion protection was improved and current density decreased from 112 to 13 nA/cm^2 for FA in comparison to HA. Also, the EIS results demonstrated that FA coating on 316 L leads to create a physical obstacle for hindering the corrosion process.
- According to the achieved results FA75 was introduced as a proper composition in view point of biocompatibility and FA coating could be considered as corrosion shield candidate.

Data availability

The raw data are available by sending an email to the corresponding authors.

Acknowledgments

The authors gratefully acknowledge the financial support provided by Isfahan University of Technology and Nikceram Razi Co. for the current study. The sincere appreciation of the authors devoted to Nanjing Forestry University for the unconditional support in the current research. Also, we would like to express our gratitude to Neda Bahremandi, Mariam Mistrom and Oisin Clancy in Lund University (Sweden) for their great communication in English language editing and prepare this article.

References

[1] V. Perrotti, F. Iaculli, A. Fontana, A. Piattelli, G. Iezzi, A.B.T.B.R.t.D.I.M Piattelli (Ed.), Intoduction of Bone Response to Dental Implant Materials, Woodhead Publishing, 2017, pp. 1–23.
[2] Dental Applications of Nanotechnology, 11 Springer, Gewerbestrasse, 2018, p. 6330 Cham, Switzerland.
[3] M. Ebrahimi, I. Mobasherpour, H.B. Bafrooei, F.S. Bidabadi, M. Mansoorianfar, Y. Orooji, A. Khataee, C. Mei, E. Salahi, T. Ebadzadeh, Taguchi design for optimization of structural and mechanical properties of hydroxyapatite-alumina-titanium nanocomposite, Ceram. Int. 45 (2019) 10097–10105.
[4] E. Kazuyoshi, T. Kogure, H. Nagasawa, Enhancement of Bone Tissue Repair by Octacalcium Phosphate Crystallizing into Hydroxyapatite In Situ, Biomineralization: From Molecular and Nano-Structural Analyses to Environmental Science, Gateway East, Singapore, (2018) 978-981-13-1002-7189721.
[5] B. Viswanath, R. Raghavan, U. Ramamurty, N. Ravishankar, Mechanical properties and anisotropy in hydroxyapatite single crystals, Scr. Mater. 57 (2007) 361–364.
[6] A.K. Mishra, Sol-Gel Based Nanoceramic Materials: Preparation, Properties and Applications 11 Springer, Gewerbestrasse, 2017, p. 6330 Cham, Switzerland, 9783319495125.
[7] E. Mohammadi Zahrani, M.H. Fathi, A.M. Alfantazi, Sol-gel derived nanocrystalline fluoridated hydroxyapatite powders and nanostructured coatings for tissue engineering applications, Metall. Mater. Trans. A: Phys. Metall. Mater. Sci. 42 (2011) 3291–3309.
[8] F. Pahlevanzadeh, H.R. Bakhsheshi-Rad, E. Hamzah, In-vitro biocompatibility, bioactivity, and mechanical strength of PMMA-PCL polymer containing fluorapatite and graphene oxide bone cements, J. Mech. Behav. Biomed. Mater. 82 (2018) 257–267.
[9] K.A. Gross, K.A. Bhadang, Sintered hydroxyfluorapatites. Part III: sintering and resultant mechanical properties of sintered blends of hydroxyapatite and fluorapatite, Biomaterials 25 (2004) 1395–1405.
[10] P. Nasker, M. Mukherjee, S. Kant, S. Tripathy, A. Sinha, M. Das, Fluorine substituted nano hydroxyapatite: synthesis, bio-activity and antibacterial response study, Ceram. Int. 44 (2018) 22008–22013.
[11] K. Fu, S. Wang, G. Wang, Y. Wang, The effects of calcium oxide on fluorapatite crystal morphology and mechanical property of functional glass-ceramics, Ceram. Int. 44 (2018) 20531–20538.
[12] M. Wei, J.H. Evans, T. Bostrom, L. Grøndahl, Synthesis and characterization of

hydroxyapatite, fluoride-substituted hydroxyapatite and fluorapatite, J. Mater. Sci. Mater. Med. 14 (2003) 311–320.
[13] K. Cheng, W. Weng, H. Wang, S. Zhang, In vitro behavior of osteoblast-like cells on fluoridated hydroxyapatite coatings, Biomaterials 26 (2005) 6288–6295.
[14] H.W. Kim, H.E. Kim, J.C. Knowles, Fluor-hydroxyapatite sol-gel coating on titanium substrate for hard tissue implants, Biomaterials 25 (2004) 3351–3358.
[15] S. Zhang, G. Liu, H. Chai, Y.-d. Zhao, L. Yu, W. Chen, Electrochemistry Communications Detection of alkaline phosphatase activity with a functionalized nanopipette, Electrochem. Commun. 99 (2019) 71–74.
[16] D. Zaffe, Some considerations on biomaterials and bone, Micron 36 (2005) 583–592.
[17] L. Krook, R.R. Minor, Fluoride and alkaline phosphatase, Fluoride 31 (1998) 177–182.
[18] M. Rockville, Bone Health and Osteoporosis: A Report of the Surgeon General, U.S. Department of Health and Human Services, Office of the Surgeon General, 2004.
[20] U.V. Natarajan, S. Rajeswari, Influence of calcium precursors on the morphology and crystallinity of sol-gel derived hydroxyapatite nanoparticles, J. Cryst. Growth 310 (2008) 4601–4611.
[21] H. Eshtiagh-Hosseini, M.R. Housaindokht, M. Chahkandi, Effects of parameters of sol-gel process on the phase evolution of sol-gel-derived hydroxyapatite, Mater. Chem. Phys. 106 (2007) 310–316.
[22] Y. Su, C. Luo, Z. Zhang, H. Hermawan, D. Zhu, J. Huang, Y. Liang, G. Li, L. Ren, Bioinspired surface functionalization of metallic biomaterials, J. Mech. Behav. Biomed. Mater. 77 (2018) 90–105.
[24] J. Sonamuthu, S. Samayanan, A.R. Jeyaraman, B. Murugesan, B. Krishnan, S. Mahalingam, Influences of ionic liquid and temperature on the tailorable surface morphology of F-apatite nanocomposites for enhancing biological abilities for orthopedic implantation, Mater. Sci. Eng. C 84 (2018) 99–107.
[25] P. Nasker, A. Samanta, S. Rudra, A. Sinha, A.K. Mukhopadhyay, M. Das, Effect of fluorine substitution on sintering behaviour, mechanical and bioactivity of hydroxyapatite, J. Mech. Behav. Biomed. Mater. 95 (2019) 136–142.
[26] M. Mansoorianfar, A. Khataee, Z. Riahi, K. Shahin, M. Asadnia, A. Razmjou, A. Hojjati Najafabadi, C. Mei, Y. Orooji, D. Li, Scalable fabrication of tunable titanium nanotubes via sonoelectrochemical process for biomedical applications, Ultrason. Sonochem. (2019) 104783, https://doi.org/10.1016/j.ultsonch.2019.104783.
[27] M. Rivas, L.J. del Valle, P. Turon, J. Puiggalí, C. Alemán, Influence of the atmosphere conditions in the structure, properties and solubility of fluorine-substituted hydroxyapatites, Mater. Chem. Phys. 226 (2019) 279–289.
[28] M. Mansoorianfar, M. Tavoosi, R. Mozafarinia, A. Ghasemi, A. Doostmohammadi, Preparation and characterization of TiO2 nanotube arrays on Ti6Al4V surface for enhancement of cell treatment, Surf. Coat. Technol. 321 (2017) 409–415.
[29] M. Mansoorianfar, M.A. Shokrgozar, M. Mehrjoo, E. Tamjid, A. Simchi, Nanodiamonds for surface engineering of orthopedic implants: Enhanced biocompatibility in human osteosarcoma cell culture, Diam. Relat. Mater. 40 (2013) 107–114.
[30] S.B.H. Farid, Osteoinduction, osteoconduction, and osseointegration, in: S.B.H. Farid (Ed.), Bioceramics: for Materials Science and Engineering, Woodhead Publishing, 2019, pp. 77–96.
[31] H.W. Kim, Y.M. Kong, C.J. Bae, Y.J. Noh, H.E. Kim, Sol-gel derived fluor-hydroxyapatite biocoatings on zirconia substrate, Biomaterials 25 (2004) 2919–2926.
[32] Y. Oshida, Y. Guven, Biocompatible coatings for metallic biomaterials, in: C. Wen (Ed.), Surface Coating and Modification of Metallic Biomaterials, Woodhead Publishing, 2015, pp. 287–343.
[33] M.H. Fathi, E.M. Zahrani, Fabrication and characterization of fluoridated hydroxyapatite nanopowders via mechanical alloying, J. Alloy. Comp. 475 (2009) 408–414.
[34] M.N. Capela, D.M. Tobaldi, C. Oliveira, A. Pereira, A.S. Duarte, M.P. Seabra, M.H.V. Fernandes, Bioactivity and antibacterial activity against E-coli of calcium-phosphate-based glasses: Effect of silver content and crystallinity, Ceram. Int. 43 (2017) 13800–13809.
[35] M. Moraveji, N. Nezafati, M. Pazouki, S. Hesaraki, Bioorthogonal surface modified α-TCP-based bone filler for enhancement of apatite formation and bioactivity, Ceram. Int. 45 (2019) 5981–5986.
[36] H.H. Beherei, G.T. El-Bassyouni, K.R. Mohamed, Modulation, characterization and bioactivity of new biocomposites based on apatite, Ceram. Int. 34 (2008) 2091–2097.
[37] M. Karimi, M.R. Ramsheh, S.M. Ahmadi, M.R. Madani, M. Shamsi, R. Reshadi, F. Lotfi, Reline-assisted green and facile synthesis of fluorapatite nanoparticles, Mater. Sci. Eng. C 77 (2017) 121–128.
[38] P. Altinci, M. Mutluay, L. Tjäderhane, A. Tezvergil-Mutluay, Effect of calcium fluoride on the activity of dentin matrix-bound enzymes, Arch. Oral Biol. 96 (2018) 162–168.
[39] S.A. Skoog, G. Kumar, R.J. Narayan, P.L. Goering, Biological responses to immobilized microscale and nanoscale surface topographies, Pharmacol. Ther. 182 (2018) 33–55.
[40] J. Mitra, G. Tripathi, A. Sharma, B. Basu, Scaffolds for bone tissue engineering: role of surface patterning on osteoblast response, RSC Adv. 3 (2013) 11073.
[41] N.S. Manam, W.S.W. Harun, D.N.A. Shri, S.A.C. Ghani, T. Kurniawan, M.H. Ismail, M.H.I. Ibrahim, Study of corrosion in biocompatible metals for implants : a review, J. Alloy. Comp. 701 (2017) 698–715.
[42] W.S.W. Harun, R.I.M. Asri, J. Alias, F.H. Zulki, K. Kadirgama, S.A.C. Ghani, J.H.M. Shari, A comprehensive review of hydroxyapatite-based coatings adhesion on metallic biomaterials, Ceram. Int. 44 (2) (2018) 1250–1268.